Carbohydrate Polymers 88 (2012) 1172–1176

Contents lists available at SciVerse ScienceDirect

Carbohydrate Polymers

journal homepage: www.elsevier.com/locate/carbpol

The interaction in sorbitol-plasticized starch bionanocomposites via positron annihilation lifetime spectroscopy and small angle X-ray scattering

Huihua Liu[a,*], Deeptangshu Chaudhary[b], Jason Roberts[c], Ryan Weed[c], James Sullivan[c], Stephen Buckman[c]

[a] School of Health Sciences, University of Ballarat,Australia
[b] Department of Chemical Engineering, Curtin University, Perth, WA, 6102, Australia
[c] ARC Centre of Excellence for Antimatter-Matter Studies (CAMS), Research School of Physics and Engineering, Australian National University, Canberra, 0200, Australia

ARTICLE INFO

Article history:
Received 10 October 2011
Received in revised form 20 January 2012
Accepted 20 January 2012
Available online 28 January 2012

Keywords:
Starch
Nanocomposite
PALS
SAXS
XRD

ABSTRACT

We investigated the free volume variations (size and distribution) within sorbitol plasticized high amylose bionanocomposites of different formula where the interactions among sorbitol, amylose and hydrophilic montmorillonite nanoclay (MMT) modified the crystallinity and therefore, the free volume of the matrix. Positron Annihilation Lifetime Spectroscopy (PALS) is a useful technique to monitor the changes of free volume within the polymer matrix – due to polymer–plasticizer or polymer–polymer interactions. In a recent investigation (Liu et al., Carbohydrate Polymer, 2011, 85(1), 97–104), we demonstrated that there exists a threshold plasticizer concentration – above which the matrix crystallinity and moisture content can be significantly altered. By investigating the relationship between the changes of free volume and the development of crystalline morphology, we presented evidence that, at the molecular level, the free volume changes due to amylose–MMT interactions were affected by the concentration of the sorbitol plasticizer. The free volume analysis revealed that when the concentration of sorbitol was low (5 wt%), the bionanocomposite showed a bimodal distribution for free volume pore-size. As the sorbitol concentration increased, these free volume pores coalesced. Further, due to sorbitol's hydrophilic nature, this study also presented the evidence of moisture 'lock-in' within the bionanocomposites matrix; only one pore size – was confirmed in the high moisture content samples; meaning that sorbitol was able to have binary interactions with the amylose and with the water molecules so that the free volume pore-size was relatively more uniform.

1. Introduction

The mechanism of molecular interaction of biodegradable starch-based nanocomposite is still a poorly understood area which has attracted many researchers. It is now well-known that the commercialization of starch-based bionanocomposites in various applications from low grade packaging to high grade cosmetics is limited by its relatively high glass transition (T_g) and humidity-sensitivity. Both these aspects are closely related to the molecular level interactions of amylose–amylose hydrophilic nature and/or amylose–plasticizer interactions. Several papers emphasizing the hydrophilic interactions between starches and various additives (including water and other plasticizers) clearly indicate the complex molecular interactions within the amylose bionanocomposites system; where water and plasticizer molecules compete with each other to occupy the free volume available within the coalescing polymer chains (Chaudhary & Adhikari, 2010; Chaudhary, Adhikari & Kasapis, 2011; Roussenova, Murith, Alam & Ubbink, 2010). With the addition of inorganic additives, such as montmorillonite nanoclay (MMT), the crystallinity of the bionanocomposites can be manipulated, and this affects the humidity-sensitivity and the T_g of the matrix, as we have demonstrated in our recent works with both glycerol and sorbitol plasticizers (Liu, Chaudhary & Tadé 2011; Liu, Chaudhary, Yusa & Tadé, 2011).

Based on the free-volume plasticization theory, the change to free volume in a plasticized polymer system is directly related to the molecular interactions within the matrix. As a result of these interactions, the arrangement of the polymeric network will be altered, and this can influence the available free sites within the polymeric system. Consequently, smaller molecules (water or plasticizer) could roam between the free volume sites of the polymer chains, thus induced changes in the crystalline domain and

---

* Corresponding author at: Mt Helen Campus, Ballarat, Vic, 3353, Victoria, Australia. Tel.: +61 353279942; fax: +61 35327 9240.

E-mail addresses: Huihua.liu@postgrad.curtin.edu.au, hliu@ballarat.edu.au (H. Liu), d.chaudhary@curtin.edu.au (D. Chaudhary), jxr107@physics.anu.edu.au (J. Roberts), rxw107@rsphysse.anu.edu.au (R. Weed), james.sullivan@anu.edu.au (J. Sullivan), stephen.buckman@anu.edu.au (S. Buckman).

0144-8617/$ – see front matter © 2012 Elsevier Ltd. All rights reserved.
doi:10.1016/j.carbpol.2012.01.069

the glass transition behavior (Chaudhary, 2010; Chaudhary et al., 2011; Chivrac, Pollet, Dole & Avérous, 2010). Positron annihilation lifetime spectroscopy (PALS) is an important technique for measuring polymer free volume (Donald, 2001) and has been applied in polymer science with the aim to understand free-volume related phenomena (Chaudhary et al., 2011; Dlubek et al., 2002; Dlubek, Shaikh, Krause-Rehberg & Paluch, 2007; Dong et al., 2008; Sharma, Roudaut, Fabing & Duplâtre, 2010; Townrow, Kilburn, Alam & Ubbink, 2007). In polymer studies, two important parameters are measured by PALS; the lifetime of ortho-positronium (oPs), τ, and the intensity of the oPs signal, I. These parameters are related to the mean free volume "cavity" radius, for example the unoccupied space between and along polymer chains, and the relative concentration of such sites, respectively. Because of its established capability in measuring pore-size of the free volume "cavity", PALS was used to investigate the influence of sorbitol concentration on the pore-size and also on the pore volume distribution within the matrix in this study. Furthermore, these changes are then related to the changes of the polymeric morphology that measured through small angle X-ray scattering (SAXS). Together with our previous publications, by studying morphological development with variation in plasticizer concentration, and by investigating changes in the molecular free volume, this report presents evidence of ternary interactions among starch/MMT/plasticizer that cause free volume changes at the molecular level, which then translate into changes in the crystallinity value, at the bulk level.

2. Materials and method

2.1. Materials and extrusion

High amylose starch (70% amylose as assayed by the company) is purchased from National Starch Company (New Jersey, USA); sorbitol is obtained from Food Department, Melbourne Company (Melbourne, Australia); Na$^+$-montmorillonite nanoclay (MMT, 99.5%) is generously supplied by NichePlas Ltd. (Sydney, Australia). Six samples were prepared at different ratios of MMT/sorbitol via extrusion (please refer to our previous publication (Liu, Chaudhary, Yusa, et al., 2011) for detailed processing parameters). In order to study the role of water molecules, two sets of sample are prepared, the as-proceeded samples and the oven-dried (12 h at 60 °C) samples. Nomenclature used here such as S305 and OS305, where 'O' refers to low moisture content samples only, 'S' refers to the sorbitol plasticizer, and 3 refers to weight percentage (wt%) of MMT (S3 means 3 wt% MMT). The last two digitals '05' refer to the wt% of sorbitol within the samples. The oven-drying treatment can remove most of the free moisture within the samples. The water content was measured by a moisturemeter (CA-100, Mitsubishi, Japan); the averaged value from three measurements was recorded. Both sets of the sample are hermetically vacuumed sealed in polyethylene bags before PALS and SAXS testing.

2.2. Positron annihilation lifetime spectroscopy

Positrons were implanted at an energy of 5 keV which ensured that surface effects were minimized. With a density of 1.2 g/cc positrons penetrate into the sample up to 1500 nm (Fig. 1). Each measurement consisted of 1×10^6 detected annihilation events and took approximately 5 h of measurement time. A fitting routine convoluted an instrument function spectrum with a series of lifetimes to determine the best parameters using the in-house developed program, CAMSFIT V2.1. Fitting variable lifetimes is typically done with 2–5 lifetimes and returns discrete results. A fixed lifetime fit is typically done with 150 lifetimes and is able to return a distribution. It was found the results from the two analysis techniques agreed closely, giving confidence in the lifetime and weight determinations.

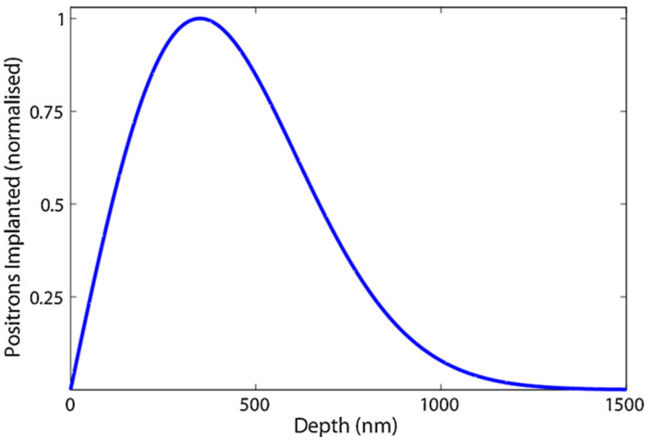

Fig. 1. Positron implantation profile at 5 keV with a density of 1.2 g/cc.

2.3. Small angle X-ray scattering (SAXS)

Small angle X-ray scattering (SAXS) was carried out at Beamline BL40B2 of Spring-8 synchrotron facility in Hyogo, Japan (Fischer, 2003). The beam was monochromatized to a wavelength of 0.1 nm with an object distance of 1151.767 mm. All the patterns recorded on CCD camera were calibrated by the diffraction rings from AgBH (Silver Behenate) standard sample. One aluminum filter block was employed to decrease the strength of X-ray for obtaining optimized experimental patterns. The measurement time per sample was chosen to eliminate the radiation damage; the optimal time was determined to be 10 s. The diffraction profiles were normalized to the beam intensity and corrected considering the empty sample background. The data reduction of obtained 2-D X-ray scattering patterns were completed with NIKA macros (Chu & Hsiao, 2001) based on Igor (Wavemetrics, Lake Oswego, Oregon). The 2-D raw scattering pattern was divided into six vectors and then averaged Q vector vs intensity plot was recorded for further analysis (Sullivan et al.,2010).

3. Results and discussion

Moisture control within the bulk starch-based materials is one of the key aspects since the bulk mechanical properties are directly related to the behavior and/or interactions of the water molecules within the matrix (Chaudhary & Adhikari, 2009; Mathew & Dufresne, 2002; Peng, Chen, Wu & Jiang, 2007). The significance of water molecules lie in their ability to influence the flexibility of the matrix, because water molecules can easily migrate within the free volume cavities (pores) and lower the T_g, especially when smaller molecular weight hydrophilic plasticizers are presented. To complicate the scenario, matrix flexibility is also influenced by the nature of plasticizer–amylose interactions and how would such interactions modify the free volume and the water content of the matrix. Because the bulk material can be investigated with techniques such as X-ray diffraction, we comprehensively studied the nucleation and growth of crystalline domains in sorbitol-plasticized amylose nanocomposites via SAXS and calorimetric analysis (Liu, Chaudhary, Ingram & John, 2011). In brief, the results pointed to an interesting behavior; the presence of plasticizer molecules helped maintain long range order and allowed greater heterogeneity to develop within the polymeric network, but the nucleation and the ensuing packing of the crystalline domains were predominantly influenced by the strong interaction of starch–MMT particles (Liu, Chaudhary, Ingram, et al., 2011). Further, based on

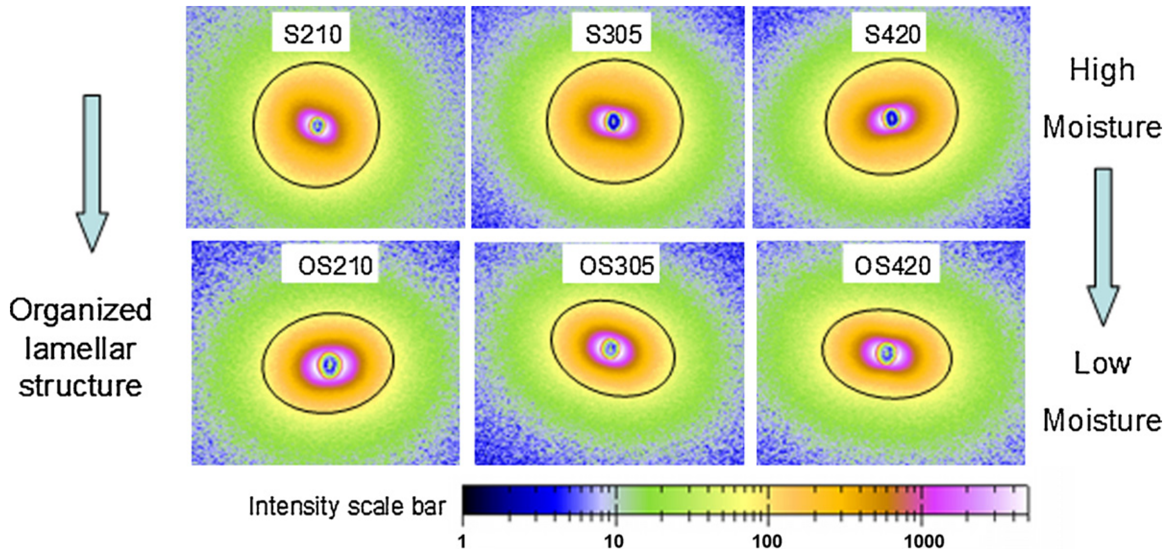

Fig. 2. 2-D scattering patterns for representative samples at different hydration degree.

the 'restricted moisture re-distribution' suggestion by Schiraldi, Piazza and Riva (1996), we also put forward the 'bridging-effect' of water molecules; where a certain concentration of water molecules was needed to allow amylose–sorbitol to link and therefore, prevent any large scale re-crystallization of amylose network (in other words, hindering the formation of large lamellar structure). The SAXS results shown in Fig. 2, based on the 2-D scattering patterns from Synchrotron SAXS analysis, supported the hypothesis of organization of the lamellar structure. Furthermore, the ellipticity of the scattering patterns, which increases upon dehydration of the sample, indicated that the large scale reorganization was possible once some water molecules are lost, and the interactions of the amylose–water are dominated by amylose–sorbitol with increase in the content of sorbitol plasticizer.

The starch–plasticizer–MMT system is a competitive system where starch–plasticizer, plasticizer–MMT, and starch–MMT interactions co-exist (Chaudhary, Torley, Halley, McCaffery & Chaudhary, 2009; Chaudhary, 2010). Thus, the structure and organization of the crystalline domains within the MMT/starch/plasticizer polymeric network is influenced by the concentration and characteristic (hydrophilic or not) of the components (Chaudhary, 2010; Chaudhary et al., 2011; Chivrac, Angellier-Coussy, Guillard, Pollet & Avérous, 2010). As shown in Fig. 2, the SAXS results qualitatively indicated the obvious changes in lamella structure and crystalline domain size; however it cannot provide a quantitative data of the free volume changes results from the crystalline rearrangements. The changes in crystalline domains size, lamellar structure, and the reorganization of the polymeric network are linked to an important system parameter – the matrix free-volume. Since there is a lack of investigation into how the plasticizer concentration and the amylose–plasticizer interaction alter the free volume distribution of the matrix, this study focused on the free volume changes using PALS, a direct free volume measurement tool, on this bionanocomposites system. Table 1 shows the PALS measurement results of the different molecular pore sizes within the bionanocomposite samples with different moisture content. For the data tabulated in Table 1, short lifetime components have been converted to pore radii using the Tao–Eldrup model, while longer components have been converted using the Rectangular Tao–Eldrup model (Kakudo & Kasai, 1972).

3.1. Interaction of sorbitol plasticizer and free volume

Table 1 indicates two interesting aspects of the free volume pore sizes within the bionanocomposites. First, the free volume available (average void radius) is larger for the high moisture samples than those of the low moisture samples, regardless of the plasticizer or MMT concentration. Since the free volume is modeled as a sphere (based on the TE model), the reduction in the free volume diameter suggested that upon removal of the water molecules the crystalline lamella network tended to grow to a denser packing within the polymeric network.

The OS305 sample with the lowest plasticizer content – 5 wt% – demonstrated a larger lifetime component (~7 nm), Table 1, with relatively small annihilation fraction (about 3% compared to the shorter lifetime weight% at ~13%), corresponding to a smaller volume fraction (although the weights cannot be directly related to the open volume fraction in this case). This is typical of amylose retrogradation due to low plasticizer content that resulted in fewer nucleation sites, and larger crystalline lamella structures. Results shown in Figs. 3 and 4 are used to discuss a 'tightly packed' MMT/starch/plasticizer polymeric network structure formed in high-sorbitol loading samples supporting by the XRD and PALS results.

Table 1
PALS measurement results for selected samples.

Sample ID	Moisture content (%)	Lifetime[a] (ns)	Void radius (nm)	Weight (%)	Lifetime[b] (ns)	Void radius (nm)	Weight (%)
S305	27.95	1.55	0.24	12.16	–	–	–
S210	28.46	1.49	0.23	14.68	–	–	–
S420	25.61	1.97	0.28	11.53	–	–	–
OS305	3.52	1.38	0.22	14.19	7.8	0.60	2.93
OS210	3.23	1.29	0.21	14.70	–	–	–
OS420	2.07	1.37	0.22	13.27	–	–	–

[a] Short lifetime components have been converted to pore radius using the Tao–Eldrup model.
[b] Long lifetime components have converted using the Rectangular Tao–Eldrup model.

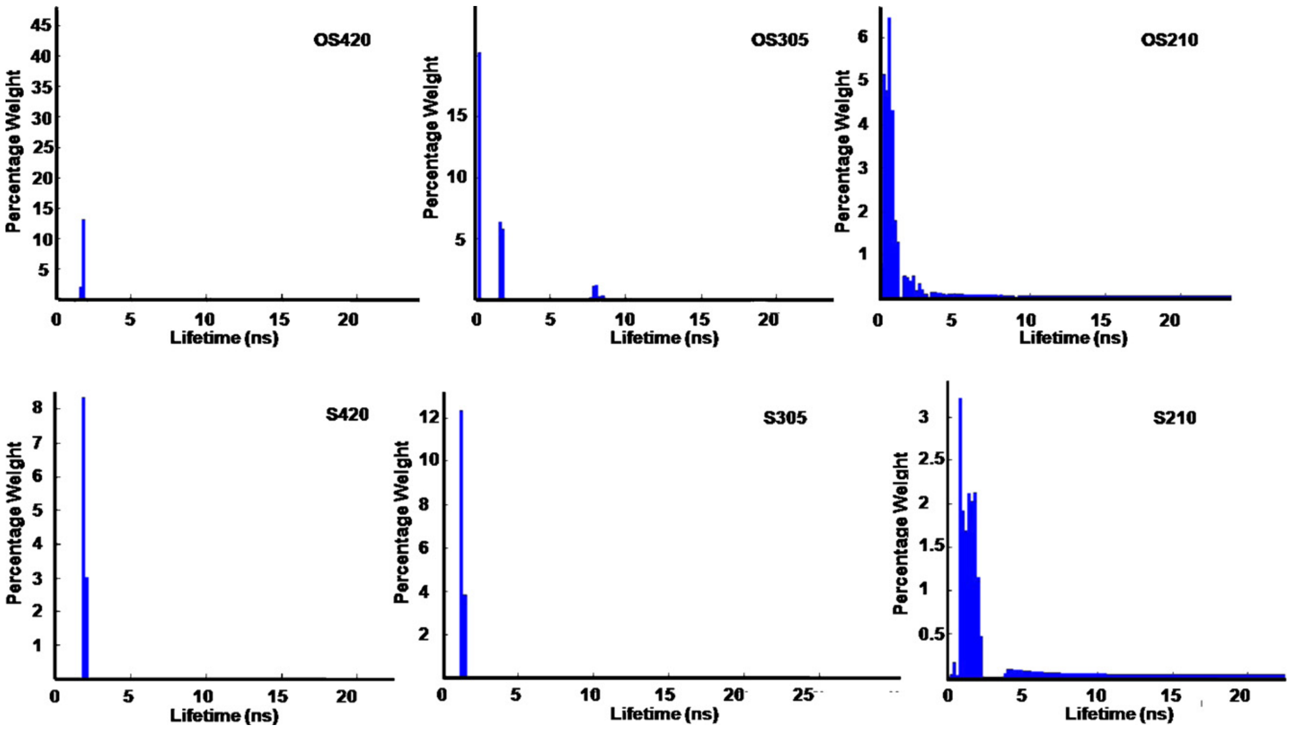

Fig. 3. PALS results for different samples.

3.2. Effect of sorbitol concentration

As described above, only OS305 showed a longer lifetime component, indicating two distinct pore size domains. As the sorbitol content increased, only one dominant lifetime was detected in the samples. It is suggested that higher quantities of sorbitol would promote larger number of nucleating sites – through greater sorbitol–MMT interaction – allowing only smaller crystalline domains to evolve. As the crystalline domain grew, they were able to squeeze the water molecules locked within the matrix. This altered the water activity of the system, and in fact, Duncan et al. reported similar observations for a simple water/carbohydrate system where new void structures within the matrix appeared depending upon the sample water activity (Alexander, 1969).

Fig. 3 showed that for all samples (both the high and low moisture samples) there is a characteristic void space of around 0.24 nm radius with an annihilation weight of about 10–15%. For the high sorbitol content, the very large lifetimes are non-existent. This is most likely due to the greater polymer/sorbitol interaction and increased mobility of the polymer chains, which allows polymer chains to occupy a greater portion of the free volume available. In other words, in the absence of water molecules, the sorbitol concentration strongly influenced the crystalline arrangement and therefore, influenced the free volume distribution. The PALS analysis of the sorbitol-plasticized samples also showed very short lifetime component (not shown here), at 0.2–0.3 ns, which is at the lower limit of our current measurement capabilities due to the temporal size of the pulse. Therefore, these very short lifetime component were considered part of the instrument function for this analysis (Sullivan et al.,2010).

Fig. 4 allowed us to compare the packing characteristics of crystalline domains in sorbitol-rich and sorbitol-poor samples, as evidenced from the shape of their d_{001} peak (Cooke & Gidley, 1992). As discussed, OS210 and OS420 showed a closely packed molecular morphology; it is interesting that this is also supported by the moisture content data where the m% of samples with packed morphologies is lower than that of the rest of the samples, Table 1. Furthermore, based on the theory of crystallography, the shape of the diffraction peak (not the 2 theta position, which indicated the distance) could be a reflection of the molecular packing of the crystalline organization. Therefore, it is worthy to note the expected broadening of d_{001} peak in OS305.This strongly suggests the formation of a less ordered MMT/starch/plasticizer polymeric network and this could be corroborated by considering the larger lifetime component (7.8 ns), corresponding to a larger void (0.60 nm) within the OS305 samples. The peak broadening behavior was also seen in the 10% sorbitol samples, albeit very small, and this highlighted that with increasing sorbitol content, the sorbitol–amylose interactions compete with the amylose–water interactions, resulting in a mixed crystalline morphology and a distribution of the free volume radii (Fig. 3, samples S210, OS210). Finally, this behavior was overcome when the sorbitol was in excess and the smaller crystalline

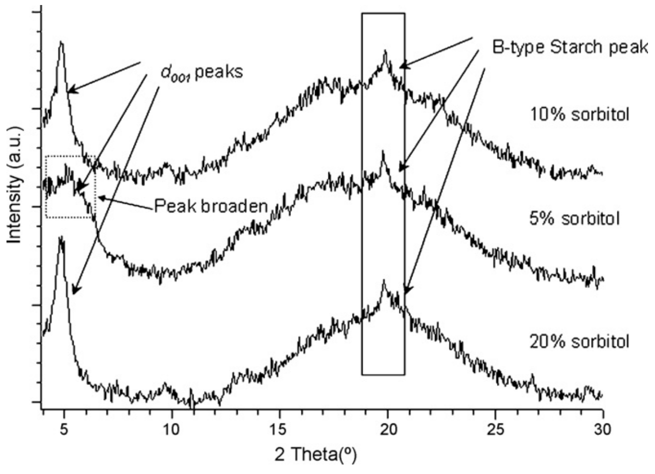

Fig. 4. XRD patterns of sorbitol-plasticized samples at different sorbitol concentrations.

Reproduced from Liu, Chaudhary & Tadé (2011).

domains were able to coalesce and develop greater orderness in its structure (sharp and narrow d_{001} peak for 20% sorbitol samples in Fig. 4).

4. Summary

The observations that the void radius within the bionanocomposite is reduced with the loss of water molecules and increased with increasing sorbitol content within the amylose-based nanocomposite allow us to conclude that the interaction between the amylose and sorbitol affects the migration of moisture and the distribution of available water molecules, influencing the polymer chain reorganization within the biopolymer network.

Based on the PALS and SAXS results presented, two morphologies can be defined; one, a MMT/starch/plasticizer polymeric network with low order of molecular arrangement and two, a MMT/starch/plasticizer polymeric network with tightly packed polymer chains. The former network is favored by low sorbitol content system and shows two different void radii which are formed based on water–amylose and sorbitol–amylose linkages. On the other hand, the latter belongs to samples with higher moisture/plasticizer content. Referring to these systems, PALS analysis shows only single void radius. In other words, the amylose organization and the formation of uniform crystalline domains are facilitated by plasticizers (both water and sorbitol) via possible 'bridging' smaller domains to form a relatively tighten uniform polymeric network.

Acknowledgments

Dr. Liu thanks the AINSE for generous financial support award. Dr. Liu would like to appreciate the support from the Self-sustaining Regions Research and Innovation Initiative, an Australian Government Collaborative Research Network (CRN) lead by the University of Ballarat. The authors would also like to acknowledge the technical support of Stephen Battisson and Ross Tranter for the experiments performed on the CAMS positron beamline. There is no potential conflict of interest between the researchers and this investigation does not bias any other investigation.

References

Alexander, L. E. (1969). *X-ray diffraction methods in polymer science*. New York: Wiley-Interscience.

Chaudhary, A. L., Torley, P. J., Halley, P. J., McCaffery, N., & Chaudhary, D. S. (2009). Amylose content and chemical modification effects on thermoplastic starch from maize – processing and characterisation using conventional polymer equipment. *Carbohydrate Polymers*, *78*(4), 917–925.

Chaudhary, D. S. (2010). Competitive plasticization in ternary plasticized starch biopolymer system. *Journal of Applied Polymer Science*, *118*(1), 486–495.

Chaudhary, D. S., & Adhikari, B. P. (2009). Glass–rubber transition of plasticised starch biopolymer affected by relative humidity. In *CHEMECA 2009* Perth, Australia, (pp. 1846–1855).

Chaudhary, D. S., & Adhikari, B. P. (2010). Understanding polymeric amylose retrogradation in presence of additives. *Journal of Applied Polymer Science*, *115*(5), 2703–2709.

Chaudhary, D. S., Adhikari, B. P., & Kasapis, S. (2011). Glass transition behaviour of plasticized starch biopolymer system – a modified Gordon–Taylor approach. *Food Hydrocolloids*, *25*(1), 114–121.

Chivrac, F., Angellier-Coussy, H., Guillard, V., Pollet, E., & Avérous, L. (2010). How does water diffuse in starch/montmorillonite nano-biocomposite materials? *Carbohydrate Polymers*, *82*(1), 128–135.

Chivrac, F., Pollet, E., Dole, P., & Avérous, L. (2010). Starch-based nano-biocomposites: plasticizer impact on the montmorillonite exfoliation process. *Carbohydrate Polymers*, *79*(4), 941–947.

Chu, B., & Hsiao, B. S. (2001). Small-angle X-ray scattering of polymers. *Chemical Reviews*, *101*(6), 1727–1762.

Cooke, D., & Gidley, M. J. (1992). Loss of crystalline and molecular order during starch gelatinisation: origin of the enthalpic transition. *Carbohydrate Research*, *227*(5), 103–112.

Dlubek, G., Pionteck, J., Bondarenko, V., Pompe, G., Taesler, C., Petters, K., et al. (2002). Positron annihilation lifetime spectroscopy (PALS) for interdiffusion studies in disperse blends of compatible polymers: a quantitative analysis. *Macromolecules*, *35*(16), 6313–6323.

Dlubek, G., Shaikh, M. Q., Krause-Rehberg, R., & Paluch, M. (2007). Effect of free volume and temperature on the structural relaxation in polymethylphenylsiloxane: a positron lifetime and pressure–volume–temperature study. *The Journal of Chemical Physics*, *126*(2), 024906.

Donald, A. M. (2001). Plasticization and self assembly in the starch granule. *Cereal Chemistry*, *78*(3), 307–314.

Dong, A. W., Pascual-Izarra, C., Pas, S. J., Hill, A. J., Boyd, B. J., & Drummond, C. J. (2008). Positron annihilation lifetime spectroscopy (PALS) as a characterization technique for nanostructured self-assembled amphiphile systems. *The Journal of Physical Chemistry B*, *113*(1), 84–91.

Fischer, H. (2003). Polymer nanocomposites: from fundamental research to specific applications. *Materials Science and Engineering: C*, *23*(6–8), 763–772.

Kakudo, M., & Kasai, N. (1972). *X-ray diffraction by polymers*. Elsevier Science & Technology.

Liu, H., Chaudhary, D. S., Ingram, G., & John, J. (2011). Interactions of hydrophilic plasticizer molecules with amorphous starch biopolymer – an investigation into the glass transition and the water activity behaviour. *Journal of Polymer Science Part B: Polymer Physics*, *49*(14), 1041–1049.

Liu, H., Chaudhary, D. S., & Tadé, M. O. (2011). Preparation and characterization of sorbitol modified nanoclay with high amylose bionanocomposites. *Carbohydrate Polymers*, *85*(1), 97–104.

Liu, H., Chaudhary, D. S., Yusa, S., & Tadé, M. O. (2011). Glycerol/starch/Na^+-montmorillonite nanocomposites: a XRD; FTIR; DSC and ^1H NMR study. *Carbohydrate Polymers*, *83*(4), 1591–1597.

Mathew, A. P., & Dufresne, A. (2002). Plasticized waxy maize starch: effect of polyols and relative humidity on material properties. *Biomacromolecules*, *3*(5), 1101–1108.

Peng, G., Chen, X., Wu, W., & Jiang, X. (2007). Modeling of water sorption isotherm for corn starch. *Journal of Food Engineering*, *80*(2), 562–567.

Roussenova, M., Murith, M., Alam, A., & Ubbink, J. (2010). Plasticization, antiplasticization, and molecular packing in amorphous carbohydrate–glycerol matrices. *Biomacromolecules*, *11*(12), 3237–3247.

Schiraldi, A., Piazza, L., & Riva, M. (1996). Bread staling: a calorimetric approach. *Cereal Chemistry*, *73*(1), 32–39.

Sharma, S. K., Roudaut, G., Fabing, I., & Duplâtre, G. (2010). Characterization of a sucrose/starch matrix through positron annihilation lifetime spectroscopy: unravelling the decomposition and glass transition processes. *Physical Chemistry Chemical Physics*, *12*, 14278–14284.

Sullivan, J., Roberts, J., Weed, R., Went, M., Newman, D., & Buckman, S. (2010). A trap-based positron beamline for the study of materials. *Measurement Science and Technology*, *21*, 085702.

Townrow, S., Kilburn, D., Alam, A., & Ubbink, J. (2007). Molecular packing in amorphous carbohydrate matrixes. *The Journal of Physical Chemistry B*, *111*(44), 12643–12648.